



ELSEVIER

Journal of Alloys and Compounds 303–304 (2000) 298–302

Journal of
ALLOYS
AND COMPOUNDS

www.elsevier.com/locate/jallcom

Magnetic properties of Dy in $\text{Pb}_2\text{Sr}_2\text{DyCu}_3\text{O}_8$

S. Skanthakumar^{a,*}, L. Soderholm^a, R. Movshovich^b^aChemistry Division, Argonne National Laboratory, Argonne, IL 60439, USA^bLos Alamos National Laboratory, Los Alamos, NM 87545, USA

Abstract

Superconductivity can be induced at high temperatures in $\text{Pb}_2\text{Sr}_2\text{RCu}_3\text{O}_8$ (R, rare earth) by partially doping Ca^{2+} for R^{3+} . In order to understand the interplay between magnetism and superconductivity, the magnetic properties of the parent compounds, $\text{Pb}_2\text{Sr}_2\text{RCu}_3\text{O}_8$, have been studied. The work presented here includes magnetic susceptibility and specific heat measurements on $\text{R}=\text{Dy}$ and extends our previous studies on $\text{R}=\text{Ce}$, Pr, Tb, Ho and Er. Specific heat experiments suggest that the Dy ions order magnetically with an ordering temperature of 1.3 K. The magnetic susceptibility data are in good agreement with the susceptibility calculated using crystal-field parameters that are extrapolated from previous modeling of the $\text{R}=\text{Er}$ and Ho analogs of this series. © 2000 Elsevier Science S.A. All rights reserved.

Keywords: High- T_c superconductors; Crystal and ligand fields; Magnetically ordered materials

1. Introduction

The valence and the magnetic properties of a rare-earth sublattice play important roles in the superconducting properties observed for the $\text{Pb}_2\text{Sr}_2\text{R}_{1-x}\text{Ca}_x\text{Cu}_3\text{O}_8$ (R, rare earth) series. These properties have been studied in detail for selected R, including Ce, Pr, Tb, Ho and Er. A variety of techniques have been used, including neutron and X-ray diffraction, inelastic neutron scattering, X-ray absorption spectroscopy, specific heat and magnetic susceptibility [1–19]. Superconductivity can be induced in $\text{Pb}_2\text{Sr}_2\text{RCu}_3\text{O}_8$ (R, rare earth) by either creating a sample with about 85% occupancy of the rare-earth site or by replacing 20–80% of the trivalent rare-earth ion with divalent Ca. This is true for all R except $\text{R}=\text{Ce}$ and Am, which have been found to be tetravalent in this series, whereas all other rare-earth ions are in the trivalent state [19,20]. The excess charge introduced by the tetravalent R is transferred to the Cu–O planes, thereby suppressing superconductivity. The $\text{R}=\text{Pr}$ analog of this series is particularly interesting [13]. $\text{Pb}_2\text{Sr}_2\text{Pr}_{0.5}\text{Ca}_{0.5}\text{Cu}_3\text{O}_8$ superconducts with slightly lower temperature than those of other rare-earth compounds. The slightly reduced superconducting transition temperature, T_c , is attributed to enhanced interactions between the Pr f-states and the CuO band states [13]. This interaction manifests itself by a relatively high antiferromagnetic ordering temperature, T_N . $\text{Pb}_2\text{Sr}_2\text{TbCu}_3\text{O}_8$ also exhibits an

enhanced T_N , but it shows no anomalous superconducting behavior [10]. One of the factors that are known to influence T_N in magnetic rare-earth oxides is the magnitude of the moment on R. Therefore, in order to understand further the magnetic interactions in the series $\text{Pb}_2\text{Sr}_2\text{RCu}_3\text{O}_8$, we have studied the magnetic behavior of the Dy analog.

Dy has a ${}^6\text{H}_{15/2}$ Russell–Saunders ground state, and is expected to have a large local moment. However, unlike the Pr and Tb analogs, Dy is not expected to have a stable tetravalent state at low energies. We report the results of magnetic susceptibility and specific heat experiments on $\text{Pb}_2\text{Sr}_2\text{DyCu}_3\text{O}_8$. Magnetic susceptibility data are in good agreement with the calculations obtained using a crystal-field model extrapolated from earlier work on the isostructural Ho and Er analogs. Specific heat measurements reveal a peak at 1.3 K, which we attribute to the long range magnetic ordering of the Dy moments in this material.

2. Experimental details

A polycrystalline sample of $\text{Pb}_2\text{Sr}_2\text{DyCu}_3\text{O}_8$ was prepared by solid-state reaction. Stoichiometric ratios of PbO, CuO, SrCO_3 and Dy_2O_3 were mixed, pelletized, and pre-fired at 750°C for 2 days. The samples were reground, pelletized and then sintered at 750°C under a N_2 atmosphere for 2 days. This procedure was repeated until the X-ray diffraction data, which were taken on a Scintag

*Corresponding author.

theta–theta diffractometer (Cu $K\alpha$ radiation), showed the sample to be single phase. X-ray diffraction room temperature data were analyzed using the General Structure Analysis System (GSAS) program [21]. The magnetization experiments were performed using a SQUID magnetometer over the temperature range of 5 to 320 K at an applied field of 500 G. Small pellets (~150 mg) of powder samples were used for this experiment. Specific heat data were collected on a 23.5 mg sample between 74 mK and 2.24 K with a quasiadiabatic technique [22,23] where ruthenium oxide thick-film resistors were used for thermometry. These thick-film ruthenium oxide resistors on clean alumina (99.5%) substrates were manufactured by State of the Art, Inc. (State College, PA, USA).

3. Results and discussion

X-ray diffraction data, which were collected between 5 and 140° at room temperature, showed the sample to be of high quality. All observed peaks can be indexed using the orthorhombic space group $Cmmm$. The absence of extra peaks in the diffraction pattern confirms the sample quality. We obtained lattice parameters of $a = 5.40127(8)$, $b = 5.44047(9)$ and $c = 15.73139(26)$ Å, in good agree-

ment with those previously reported [1]. Recent studies on $Pb_2Sr_2YCu_3O_8$ using high-resolution diffraction found that although the samples have an orthorhombic structure above 240°C , at room temperature there is a slight monoclinic distortion with a distribution of the β angle [14,19]. In those experiments, peaks (h,k,l) with both h and l nonzero are found to be broader than the other peaks. Similar behavior is also observed in $Pb_2Sr_2DyCu_3O_8$. In particular, our data indicate that the $(1,1,4)$ and $(2,0,5)$ peaks are much broader than the $(0,0,2)$, $(0,2,0)$ and $(0,2,5)$ peaks, a result similar to that found for $Pb_2Sr_2YCu_3O_8$. If there is a simple monoclinic distortion, the peaks (h,k,l) with both h and l nonzero split into two peaks (h,k,l) and $(h,k,-l)$. Even though our resolution was sufficient to resolve peaks attributable to this monoclinic distortion, the $(1,1,4)$ and $(2,0,5)$ peaks are significantly broadened, but are not observably split. The observation of a similar peak broadening for the Dy analog as for Y indicates that the monoclinic distortion reported for $Pb_2Sr_2YCu_3O_8$ occurs also in $Pb_2Sr_2DyCu_3O_8$. High-resolution X-ray data are necessary to further model this monoclinic distortion.

Magnetic susceptibility data, obtained from a powder sample and measured as a function of temperature, are shown Fig. 1. Also shown in the inset are the same data

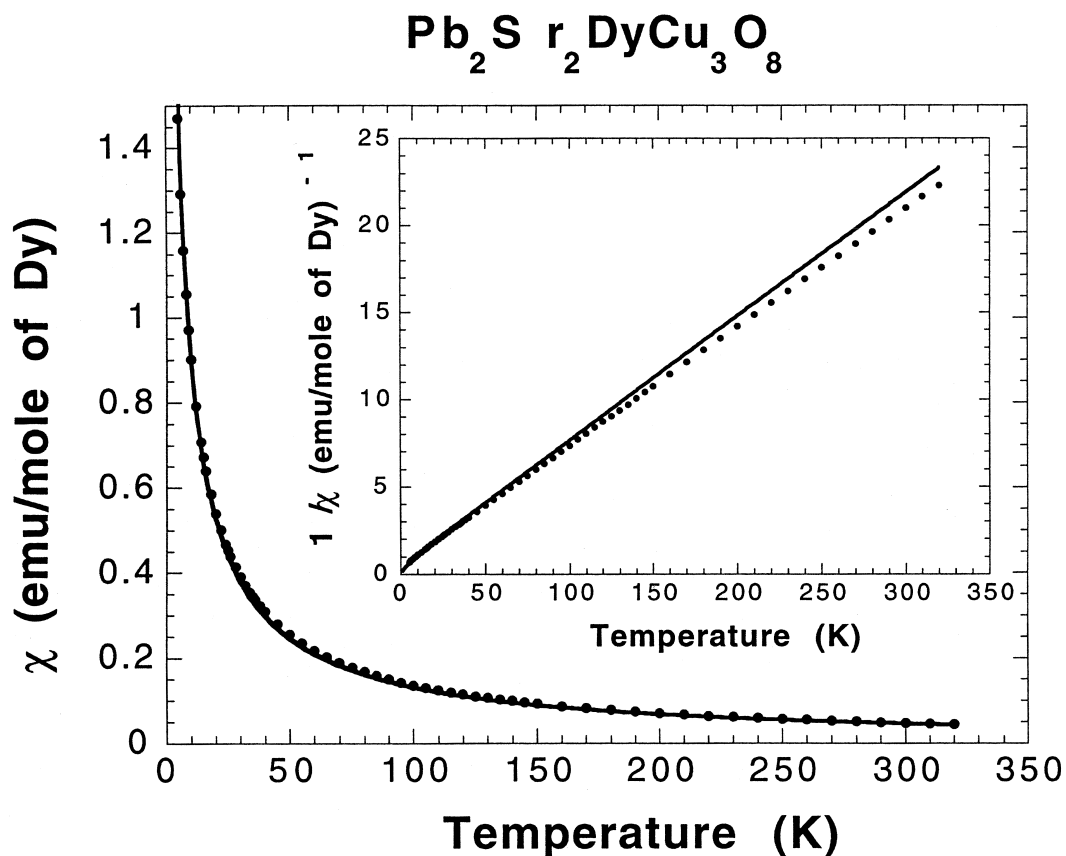


Fig. 1. Temperature dependence of the measured (symbols) magnetic susceptibility of a polycrystalline sample. The solid line is the calculated susceptibility using a crystal-field model. The same data are depicted as a Curie–Weiss plot in the inset.

depicted as a Curie–Weiss plot. There is no indication of any Dy magnetic ordering between 5 and 320 K. We fit the data to a modified Curie–Weiss law:

$$\chi = \frac{C}{T + \Theta} + \chi_{\text{TIP}} \quad (1)$$

where C and Θ are Curie and Weiss constants and χ_{TIP} is the temperature independent susceptibility. The results of our refinement are shown in Table 1. An effective moment, calculated using $\mu_{\text{eff}} = (8C)^{1/2}$, of 10.7(1) μ_{B} is determined from the high-temperature data (>150 K). This moment is the same, within error, as the free-ion moment of 10.6 μ_{B} expected for Dy^{3+} . In $\text{Pb}_2\text{Sr}_2\text{DyCu}_3\text{O}_8$, Cu spins will also contribute to the magnetic susceptibility. The magnetic behavior of Cu is not well understood in these compounds. However, the Cu contribution to the total susceptibility is expected to be small because copper's magnetic moment is significantly smaller than that of Dy, and magnetic susceptibility is proportional to the sum of the squares of the effective moments.

The magnetic susceptibility deviates significantly from Curie–Weiss behavior at low temperatures. A Curie–Weiss fit to the data (Table 1) above 5 K reduces the effective moment from 10.7 to 10.0(1) μ_{B} , which is significantly smaller than the expected free-ion moment (10.6 μ_{B}). This significant difference is attributable to either crystal-field effects or to significant exchange interactions.

In order to distinguish these two possibilities, we have calculated the single-ion magnetic susceptibility. We used a crystal-field model developed previously [16] and compared the calculated susceptibility with the experimental data. Dy ions in $\text{Pb}_2\text{Sr}_2\text{DyCu}_3\text{O}_8$ are surrounded by eight equidistant nearest-neighbor oxygen ions, to form a site with near-neighbor tetragonal symmetry. The Dy ground state properties are mainly determined by these near-neighbor oxygen ions. The slight deviation of the true crystal symmetry from tetragonal is not expected to have a significant effect on the crystal-field splitting in the Dy ground state. Therefore, we consider the Dy site symmetry to be tetragonal (D_{4h}). Using previously determined methodology and formalism [24,25], The crystal field in D_{4h}

symmetry is characterized by five parameters, B_0^2 , B_0^4 , B_0^6 , B_4^4 and B_4^6 . The crystal field will split the Dy^{3+} Russell–Saunders ${}^6\text{H}_{15/2}$ ground multiplet into 4 Γ_6 and 4 Γ_7 Kramers doublets. Further details about our crystal-field modeling can be found elsewhere [16,17]. The crystal-field parameters for $\text{Pb}_2\text{Sr}_2\text{DyCu}_3\text{O}_8$ have not been previously determined, therefore we have extrapolated a set of parameters from previous work on the Ho and Er analogs [17]. Using the extrapolated parameters $B_0^2 = 160$, $B_0^4 = -2316$, $B_0^6 = 457$, $B_4^4 = 1138$ and $B_4^6 = 1369$ cm^{-1} , the powder-averaged single-ion magnetic susceptibility was calculated for Dy^{3+} in the $\text{Pb}_2\text{Sr}_2\text{DyCu}_3\text{O}_8$ lattice. The calculated and experimental susceptibilities are compared in Fig. 1, and the inverse susceptibilities are shown in the inset. The slight deviation between the calculated and experimental inverse susceptibilities can be accounted for by a contribution from the Cu moments to the experimental data.

Our model predicts a strong magnetic anisotropy, which places the magnetic easy axis along the c crystallographic axis. The temperature dependence of the magnetic properties is not expected to strictly follow the Curie–Weiss law, particularly at very low temperatures. We have fit the calculated magnetic susceptibilities above 10 K to the Curie–Weiss law, and the results (Table 1) show a reduced moment that is in agreement with the experimental data. These results show that the crystal field has a significant effect on the single-ion magnetic properties of Dy^{3+} at low temperatures. The good agreement between the magnetic susceptibility data and our calculations confirms that the deviations from Curie–Weiss behavior at low temperatures are the result of crystal-field effects, and not significant Dy exchange interactions.

The specific heat of $\text{Pb}_2\text{Sr}_2\text{DyCu}_3\text{O}_8$, measured at low temperatures, is shown in Fig. 2. These data shows a cusp at about 1.3 K that we interpret as arising from the magnetic ordering of the Dy moments. Contributions to specific heat arise from four sources: electronic, lattice, crystal field and magnetic ordering. The electronic (linear term) and lattice-phonon contributions (cubic term) to our measurement can be estimated by comparison to a similar measurement on an isostructural analog with a nonmagnetic R, $\text{Pb}_2\text{Sr}_2\text{YCu}_3\text{O}_8$ [7]. From this comparison we conclude that there are no significant electronic or lattice contributions to the specific heat below 3 K. The crystal-field contribution to the specific heat can be calculated from the wave functions and energies of our modeled crystal-field states. Our calculation of this contribution at low temperatures is shown in Fig. 2 as a solid line. The inset in Fig. 2 shows a Schottky-like anomaly at about 20 K, which is an order of magnitude higher in temperature than the experimentally determined cusp. This result eliminates significant crystal-field contributions to the transition at 1.3 K. By this process of elimination, we conclude that the 1.3 K cusp in the specific heat data is due to the magnetic ordering of Dy^{3+} moments.

Table 1

Results of the fit (Eq. (1)) to the $\text{Pb}_2\text{Sr}_2\text{DyCu}_3\text{O}_8$ experimental and crystal-field modeled magnetic susceptibility data. The fitted region is also given. The effective moment (μ_{eff}) is calculated using $\mu_{\text{eff}} = (8C)^{1/2}$, where C is the Curie constant. The Weiss constant Θ and the temperature independent contribution χ_{TIP} are also given along with the fitted temperature region

	Temperature region	μ_{eff} (μ_{B})	Θ (K)	χ_{TIP}
Expt.	150 < T < 320 K	10.7(1)	5.8(7)	0.0008(2)
Expt.	5 < T < 320 K	10.0(1)	3.8(1)	0.0136(20)
Expt.	10 < T < 320 K	10.4(1)	5.1(1)	0.0057(8)
Calc.	10 < T < 320 K	10.3(1)	4.7(1)	0.0040(3)

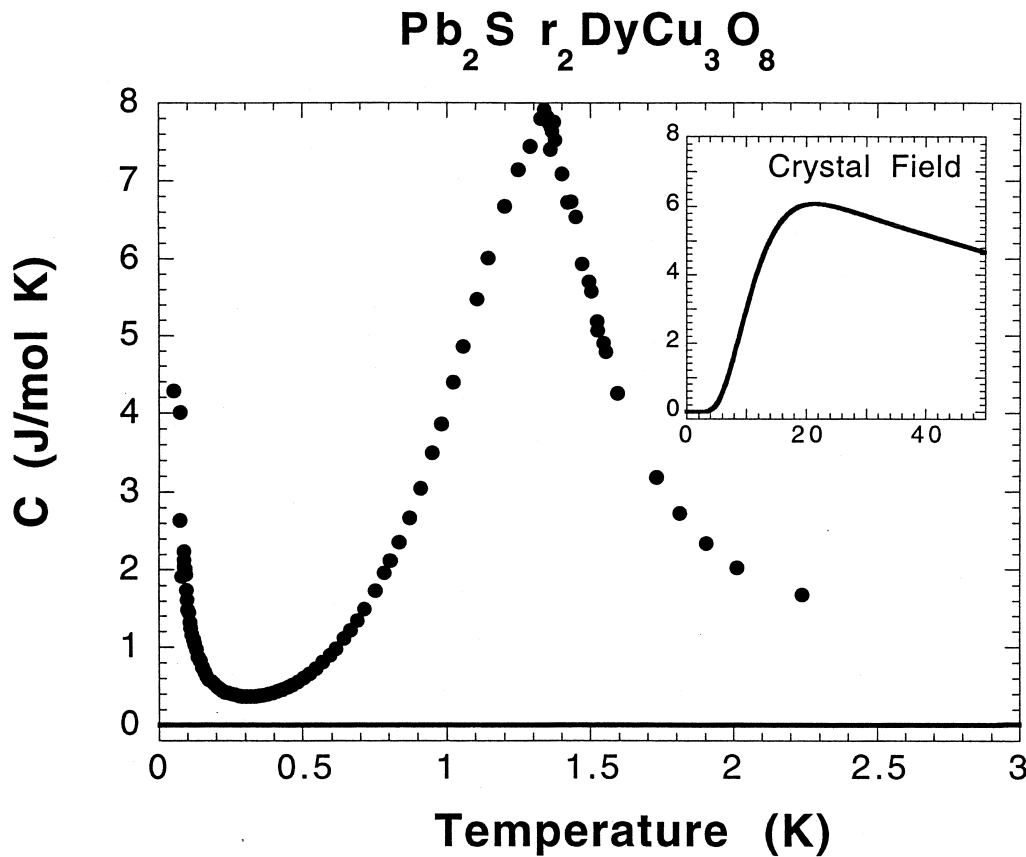


Fig. 2. Temperature dependence of the specific heat. The transition at 1.3 K originates from the magnetic ordering of the Dy moments. The calculation of the crystal-field contribution to the specific heat is shown as a solid line and in the inset over a broader range.

The high-temperature tail of the specific heat cusp extends far above the assigned transition temperature of $T_N = 1.3$ K, reflecting high-temperature fluctuations that set in well above the magnetic ordering temperature. These fluctuations may be the result of a two-dimensional character of the magnetic order, with an interaction energy that extends far above T_N , and results in the 3D ordering observed at T_N . About half of the $R \ln(2)$ entropy is released below the transition temperature of $T_N = 1.3$ K. The full $R \ln(2)$ is released below 2 K, confirming our modeling which predicted the doubly degenerate Dy electronic ground state in $\text{Pb}_2\text{Sr}_2\text{DyCu}_3\text{O}_8$. The low-temperature tail (below 0.3 K) is a manifestation of the nuclear Schottky anomaly of the magnetically ordered Dy atoms.

The Dy ions in $\text{Pb}_2\text{Sr}_2\text{DyCu}_3\text{O}_8$ have an environment similar to that in $\text{DyBa}_2\text{Cu}_3\text{O}_7$, and hence we expect the magnetic properties in these two materials to be similar. The magnetic properties of Dy in $\text{DyBa}_2\text{Cu}_3\text{O}_7$ have been studied extensively [26–34]. Antiferromagnetic ordering of the Dy moments in $\text{DyBa}_2\text{Cu}_3\text{O}_7$ occurs at $T_N \approx 0.9$ K, and dipole interactions play an important role. Although 3d magnetic ordering is observed, there is 2d-like magnetic behavior, which is observed even above the T_N . This

behavior originates naturally from the 2D-like crystal structure. The Dy–Dy nearest-neighbor distance along the c -axis (~ 11.9 Å) in $\text{DyBa}_2\text{Cu}_3\text{O}_7$ is about three times larger than that in the a – b plane (~ 3.9 Å). Therefore, Dy magnetic coupling within the a – b plane is expected to be much stronger than the coupling along the c -axis, resulting in the observed 2d behavior. The single-ion magnetic anisotropy puts the easy axis along the c -direction. Simple antiferromagnetic ordering is observed in $\text{DyBa}_2\text{Cu}_3\text{O}_7$ between the nearest neighbors in the a – b plane, as expected for dipole interactions. Indirect (RKKY) exchange interactions couple these planes along the c -axis. In $\text{Pb}_2\text{Sr}_2\text{DyCu}_3\text{O}_8$ the Dy nearest-neighbor distance along the c -axis (15.7 Å) is even longer than that in $\text{DyBa}_2\text{Cu}_3\text{O}_7$, although the distances are about the same in the a – b plane. Hence we expect a similar or more enhanced 2d magnetic behavior in $\text{Pb}_2\text{Sr}_2\text{DyCu}_3\text{O}_8$ than observed in $\text{DyBa}_2\text{Cu}_3\text{O}_7$. Our specific heat data above $T_N = 1.3$ K are consistent with this expectation. Since the crystal-field anisotropy, which was calculated from our model, predicts the c -direction as easy axis, and dipole interactions play an important role, we expect the magnetic structure in both compounds to be the same within the a – b plane. As in $\text{DyBa}_2\text{Cu}_3\text{O}_7$, the rare-earth ions are effec-

tively isolated electronically from the superconducting Cu–O planes in $\text{Pb}_2\text{Sr}_2\text{Dy}_{1-x}\text{Ca}_x\text{Cu}_3\text{O}_8$, and therefore superconductivity is not affected by the magnetic ordering of Dy in this system.

Neutron diffraction measurements on the R=Pr and Tb analogs of $\text{Pb}_2\text{Sr}_2\text{RCu}_3\text{O}_8$ also reveal 2d rare-earth magnetic behavior, with $T_N = 6.0$ and 5.3 K, respectively [5,8,11,15]. The relatively high transition temperatures in these two compounds indicate that exchange interactions, rather than dipole interactions, play an important role in the magnetic properties. Our recent specific heat measurements show similar 2d magnetic properties for R=Sm, with an ordering temperature of 1.1 K, whereas R=Nd show 3d behavior with an ordering temperature of 1.7 K [35].

In conclusion, we have studied the physical properties of $\text{Pb}_2\text{Sr}_2\text{DyCu}_3\text{O}_8$. Its crystal structure is found to be the same as that determined for other $\text{Pb}_2\text{Sr}_2\text{RCu}_3\text{O}_8$ compounds. Magnetic susceptibility measurements are in good agreement with calculations assuming a single-ion crystal-field model. Specific heat data revealed a 2d magnetic behavior with a 3d magnetic ordering at 1.3 K.

Acknowledgements

The work at Argonne (S.S., L.S.) is supported by the DOE-Basic Energy Sciences, Chemical Sciences under W-31-109-ENG-38. Work at Los Alamos (R.M.) was performed under the auspices of the Department of Energy.

References

- [1] L.F. Schneemeyer, R.J. Cava, A.C.W.P. James, P. Marsh, T. Siegrist, J.V. Waszczak, J.J. Krajewski, R.L. Opila, S.H. Glarum, J.H. Marshall, R. Hull, J.M. Bonar, *Chem. Mater.* 1 (1989) 548.
- [2] J.S. Xue, M. Reedyk, Y.P. Lin, C.V. Stager, J.E. Greedan, *Physica C* 166 (1990) 29.
- [3] J.S. Xue, J.E. Greedan, M. Maric, *J. Solid State Chem.* 102 (1993) 501.
- [4] J.S. Xue, M. Reedyk, J.E. Greedan, T. Timusk, *J. Solid State Chem.* 102 (1993) 492.
- [5] J.H. Shieh, H.C. Ku, J.C. Ho, *Phys. Rev. B* 50 (1994) 3288.
- [6] W.T. Hsieh, W.-H. Li, K.C. Lee, J.W. Lynn, J.H. Shieh, H.C. Ku, *J. Appl. Phys.* 76 (1994) 7124.
- [7] C.R. Shih, T.H. Meen, Y.C. Chen, H.D. Yang, *Phys. Rev. B* 50 (1994) 9619.
- [8] S.Y. Wu, W.T. Hsieh, W.-H. Li, K.C. Lee, J.W. Lynn, H.D. Yang, *J. Appl. Phys.* 75 (1994) 6598.
- [9] U. Staub, L. Soderholm, S. Skanthakumar, M.R. Antonio, *Phys. Rev. B* 52 (1995) 9736.
- [10] U. Staub, L. Soderholm, S. Skanthakumar, S. Rosenkranz, C. Ritter, W. Kagunya, *Europhys. Lett.* 34 (1996) 447.
- [11] U. Staub, L. Soderholm, S. Skanthakumar, S. Rosenkranz, C. Ritter, W. Kagunya, *Z. Phys. B* 104 (1997) 37.
- [12] U. Staub, S. Skanthakumar, L. Soderholm, R. Osborn, *J. Alloys Comp.* 250 (1997) 581.
- [13] U. Staub, L. Soderholm, S. Skanthakumar, R. Osborn, F. Fauth, *Europhys. Lett.* 39 (1997) 663.
- [14] U. Staub, L. Soderholm, S. Skanthakumar, P. Pattison, K. Conder, *Phys. Rev. B* 57 (1998) 5535.
- [15] U. Staub, L. Soderholm, S. Skanthakumar, R. Osborn, F. Fauth, C. Ritter (preprint).
- [16] U. Staub, L. Soderholm, in: J.K.A. Gschneidner, L. Eyring, M.B. Maple (Eds.), *Handbook on the Physics and Chemistry of Rare Earths*, Elsevier, Amsterdam (in press).
- [17] L. Soderholm, C.-K. Loong, U. Staub, S. Skanthakumar, J.S. Xue, J.P. Hammonds, J.E. Greedan, M. Maric, *Physica C* 246 (1995) 11.
- [18] L. Soderholm, S. Skanthakumar, U. Staub, M.R. Antonio, C.W. Williams, *J. Alloys Comp.* 250 (1997) 623.
- [19] S. Skanthakumar, L. Soderholm, *Phys. Rev. B* 53 (1996) 920.
- [20] L. Soderholm, C. Willaims, S. Skanthakumar, M.R. Antonio, S. Condarson, *Z. Phys. B* 101 (1996) 539.
- [21] A.C. Larson, R.B.V. Dreele, *GSAS Technical Manual*, 1994.
- [22] F.J. Morin, J.P. Maita, *Phys. Rev. B* 129 (1963) 1115.
- [23] J.C. Lasjaunias, B. Picot, A. Ravex, D. Thoulouze, M. Vandorpe, *Cryogenics* 17 (1977).
- [24] H.M. Crosswhite, H. Crosswhite, *J. Opt. Soc. Am. B* 1 (1984) 246.
- [25] B.G. Wybourne, *Spectroscopic Properties of Rare Earths*, Interscience, New York, 1965, 236 pp.
- [26] H.P.V.D. Meulen, J.J.M. Franse, Z. Tarnawski, K. Kadowaki, J.C.P. Klasse, A.A. Menovski, *Physica C* 152 (1988) 65.
- [27] Y. Nakazawa, M. Ishikawa, T. Takabatake, *Physica B* 148 (1987) 404.
- [28] A.P. Ramirez, L.F. Schneemeyer, J.V. Waszczak, *Phys. Rev. B* 36 (1987) 7145.
- [29] T.W. Clinton, J.W. Lynn, J.Z. Liu, Y.X. Jia, R.N. Shelton, *J. Appl. Phys.* 70 (1991) 5751.
- [30] T.W. Clinton, J.W. Lynn, J.Z. Liu, Y.X. Jia, T.J. Goodwin, R.N. Shelton, B.W. Lee, M. Buchgeister, M.B. Maple, J.L. Peng, *Phys. Rev. B* 51 (1995) 15429.
- [31] P. Fischer, K. Kakurai, M. Steiner, K.N. Clausen, B. Lebech, F. Hulliger, H.R. Ott, P. Brüesch, P. Unternährer, *Physica C* 152 (1988) 145.
- [32] A.I. Goldman, J. Tranquada, J.E. Crow, C.-S. Jee, *Phys. Rev. B* 36 (1987) 7234.
- [33] J.W. Lynn, *J. Alloys Comp.* 181 (1992) 419.
- [34] J.W. Lynn, S. Skanthakumar, in: J.K.A. Gschneidner, L. Eyring, M.B. Maple (Eds.), *Handbook on the Physics and Chemistry of Rare Earths*, Elsevier, Amsterdam (in press).
- [35] S. Skanthakumar, L. Soderholm, R. Movshovich (in preparation).